

Photoelectrochemical Investigation of Solar Cell Materials**

Thomas Cotting, Elisabeth Müller, Hans von Känel*, and Ruedi Hauger
Günther Leicht and Francis Lévy

This contribution deals with some principles and problems of photoelectrochemical solar energy conversion and their influence on current semiconductor materials research. Can hydrogen production by photoelectrolysis be expected to become of any importance in the future? We outline the physical principles governing the behaviour of illuminated semiconductor electrodes in aqueous electrolytes. As an example characterization of the p-type, single crystal, ternary chalcopyrites $CdSiAs_2$ and $ZnSnP_2$ is presented.

1. Introduction

Increasing air pollution and its consequences, and in the long run limited reserves demand the investigation of substitutes for the fossil fuels. Hydrogen as a fuel has many attractive features such as the possibility of either clean combustion

in engines or the direct conversion to electricity in fuel cells^[1]. Today hydrogen gas is used in large quantities in the chemical industry and is produced by reaction of natural gas (CH_4) with water or by the gasification of coal. Future large-scale hydrogen production might not depend on fossil fuels as a raw material. But the splitting of water into hydrogen and oxygen by conventional electrolysis needs a tremendous quantity of electrical energy which has to be produced first. Since the production of electricity by nuclear power has become a highly politicized topic, for the future great emphasis has to be put on the investigation of renewable energies like solar energy^[2].

There are several methods in using solar energy for water splitting. One of it is the photoelectrolysis by semiconductor electrodes. In this paper we would like to

Thomas Cotting: Born 1959. Studied physics at ETH Zürich; 1984 diploma in physics; 1984 start of a dissertation on semiconductor photoelectrochemistry at the Laboratorium für Festkörperphysik, ETHZ.

Elisabeth Müller: Born 1964. Studied physics at ETH Zürich; 1988 diploma in physics.

Hans von Känel: Born 1950. Studied physics at ETH Zürich; 1974 diploma in physics; 1974–1978 dissertation at the Laboratorium für Festkörperphysik, ETHZ. 1979–1981 post-doc at the Massachusetts Institute of Technology. Since 1981 leader of the project «Photoelectrolysis of water with semiconductor electrodes» at ETHZ.

Ruedi Hauger: Born 1930. Studied chemistry at the Universität Saarbrücken; 1961 diploma in chemistry. Employments in several companies of chemical industry. Since 1967 research associate at the Laboratorium für Festkörperphysik, ETHZ.

Günther Leicht: Born 1960. Studied physics at the Universität Konstanz; 1986 diploma in physics. Since 1986 research assistant at the Institut de physique appliquée, ETH Lausanne.

Francis Lévy: Born 1940. Studied physics at the ETH Zürich; 1963 diploma in physics; 1963–1969 dissertation at the Laboratorium für Festkörperphysik, ETHZ. 1969–1987 senior scientist at the Institut de physique appliquée, ETH Lausanne. Since 1987 Professor of Physics at EPFL.

show some basic principles and problems, and how they affect our semiconductor materials research.

2. Principles and Problems

For simplicity let us look at an electrolyte containing only one potential-controlling redox couple, e.g. $Cr^{3\oplus}/Cr^{2\oplus}$. The electrochemical potential is determined by the standard potential of this redox couple, the ratio between the concentrations of the reduced and the oxidized compo-

* Correspondence: Dr. H. von Känel
Laboratorium für Festkörperphysik
Eidgenössische Technische Hochschule Zürich
ETH-Hönggerberg, HPF F15
CH-8093 Zürich

** This article is based on a paper presented at the Workshop «Photochemical Transformation and Storage of Solar Energy; Conversion of CO_2 and Fuel Cells» in Kulturzentrum Appenberg in Zäziwil, November 9/10, 1987, organized by Prof. G. Calzaferri (Universität Bern), sponsored by the Bundesamt für Energiewirtschaft.

ment, and the temperature. The electrochemical potential of a semiconductor (i.e. the Fermi level) depends on its kind, the temperature, and the doping (Fig. 1). Upon immersing the semiconductor in the electrolyte an electrical charge exchange occurs across the interface by diffusion (diffusion current), due to the pre-

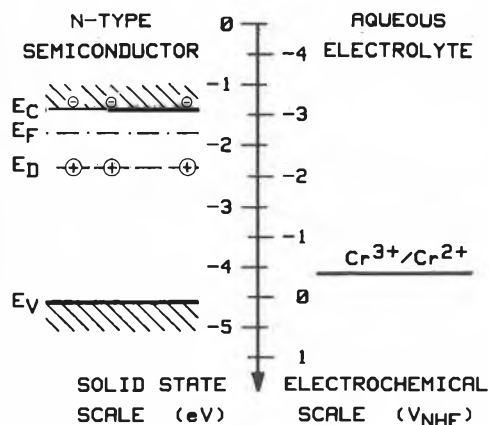


Fig. 1. Energy levels for a n-type semiconductor and an aqueous electrolyte containing the redox couple Cr^{3+}/Cr^{2+} before electrode immersion. The following abbreviations were made: E_C = lower conduction band edge, E_V = upper valence band edge, E_D = energy level of the donors, E_F = Fermi level in the semiconductor. The relation between the energy scale used in solid state physics and the electrochemical scale is approximately given by the formula: $E[eV] = -q \cdot V_{NHE} - 4.5$.

viously different electrochemical potentials. Thermodynamical equilibrium between the two phases is reached when the electrical field inside the semiconductor resulting from this charge transfer introduces a drift current which will compensate the diffusion current. The energy band scheme resulting from this semiconductor/electrolyte configuration is comparable to that one for a semiconductor/metal interface and may be treated in first order by the simple Schottky theory.

Fig. 2 illustrates the above mentioned process for a n-type semiconductor. As long as no thermodynamical equilibrium is reached, electrons diffuse from the semiconductor into the electrolyte reducing the oxidized component Cr^{3+} . Since some of the ions in the semiconductor are no longer compensated a positive space charge is left near the interface (space charge layer or depletion layer) while in the electrolyte a negative counter charge of solvated negative ions occurs (Helmholtz layer). Since the cell resistance should be small relatively high concentrated electrolytes (1M) are used and so the potential drop in the electrolyte is nearly totally localized in the Helmholtz layer.

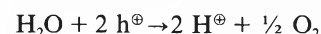
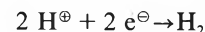
The consequence of this charge distribution is an electrical field, correlating with the depicted potential drop and energy band scheme. Since the electrodes are not metals but semiconductors the Fermi level lies between the valence band and the conduction band in the forbidden zone, called energy gap. In the case of a n-type semiconductor the Fermi level is situated near the lower conduction band edge (Fig. 1) indicating the presence of donor centers inside the energy gap near the conduction band (giving up electrons to the latter). In the case of p-type semiconductors the Fermi level lies near the upper valence band edge indicating acceptor centers near the valence band. Once all acceptors or donors are ionized additional charge carriers can only be generated by interband transition like the photogeneration of an electron-hole pair. This means that an electron in the valence band is excited by an incident photon to

the conduction band leaving behind a positively charged hole. But the energy of the photon has to be at least of the same size as the energy gap.

As we have seen the band bending depends on the inner electrical field and can therefore be influenced more or less by the choice of the redox couple.

In a photoelectrochemical solar cell consisting of a semiconductor with an ohmic back contact, an electrolyte with a redox couple, a metallic counter electrode, and a resistive load the electrical field in the space charge layer is used to separate optically generated electron-hole pairs. In the case of a n-type semiconductor the minority carriers, the holes, drift to the semiconductor/electrolyte interface where they oxidize the reduced component of the electrolyte while the electrons move through the bulk, the back contact, and the load to the counter electrode where the inverse process takes place. Since the maximal achievable photovoltage depends on the band bending in the dark a redox potential near the valence band is desirable.

The function of a photoelectrolysis cell is nearly the same. But there is not just one redox couple which can be chosen more or less at will. Instead we have two redox couples (H^+/H_2 and H_2O/O_2) with fixed redox potentials (at fixed pH). In the case of a p-type semiconductor in contact with an aqueous electrolyte optically generated minority carriers (electrons) reduce H^+ to H_2 while at the counter electrode the holes oxidize the water (Fig. 3).



3. Semiconductor Materials

For the design of a photoelectrochemical solar cell or a photoelectrolysis cell we have to know some basic parameters of the semiconductor/electrolyte interface, such as the quantum efficiency, the size and kind of the energy gap, the

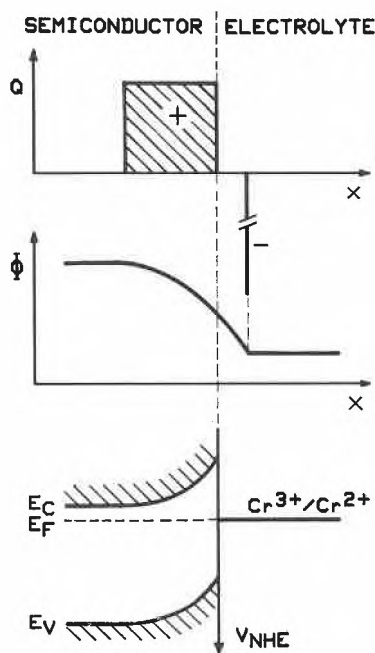


Fig. 2. Illustration of the charge distribution, the electric potential, and the band scheme (from top) after the thermodynamical equilibrium between a n-type semiconductor and an aqueous electrolyte (with Cr^{3+}/Cr^{2+}) has been reached.

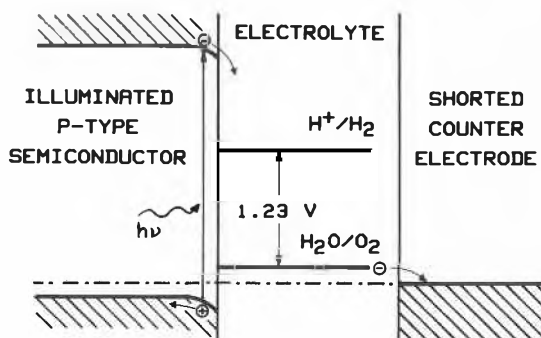


Fig. 3. Photoelectrolysis cell with a p-type semiconductor under illumination. In an ideal cell, without any external bias, the H^+/H_2 redox level lies below the conduction band edge and the H_2O/O_2 level lies above the valence band edge.

flatband potential, corrosion behaviour, etc.

Quantum efficiency:

The quantum efficiency shows the capability of a semiconductor to convert light to electricity. It is defined as the ratio between the number of incident photons and the number of produced and separated electron-hole pairs which contribute to the photocurrent.

Energy gap:

The optimal bandgap of a semiconductor in a photovoltaic device lies around 1.5 eV. An older reference gives a range of about 1.3 to 1.6 eV for a cloudy day^[3]. A new one shows that a large part of the infrared spectrum is absorbed under special conditions like covered sky what would shift the ideal bandgap to a higher value^[4]. Incident light with an energy smaller than the bandgap does not contribute to the photocurrent since it cannot lift an electron to the conduction band. On the other hand maximal band bending in the dark and hence the achievable photovoltage is higher the larger the gap. In a photoelectrolysis cell where 1.23 V for the splitting of water are required at zero current the gap energy would have to be larger than 2.3 eV with only one absorber material and without an external bias due to the large overvoltages, especially for O₂-generation^[5]. A direct optical transition (no phonons involved) is preferable since then the absorption is higher and thin film solar cells are possible.

Flatband potential:

The flatband potential is the potential which has to be applied to the semiconductor in order for the initial band bending to vanish. If this value is known, the energetics (like band bending under different redox couples) of the semiconductor/electrolyte interface can be estimated and eventually optimized by the choice of the redox couple.

Corrosion behaviour:

A main problem in semiconductor photoelectrochemistry is the photocorrosion. Specially the n-type semiconductors suffer under the selfdestroying by photooxidation while the p-type semiconductors seem to be more stable.

Good results in photoelectrochemical solar cells were achieved with semiconductors of zincblende structure like InP or GaAs which both have a direct optical fundamental but relatively small gap (1.3 eV and 1.4 eV). The close relationship between the bandstructures of zincblende and chalcopyrite semiconductors have led us to expect similar properties for the latter. In this paper we report some results of our investigations on the p-type, single crystal, ternary chalcopyrites CdSiAs₂ and ZnSnP₂. Crystal growth and preparation is described elsewhere and has not to be repeated here^[6,7].

4. Experimental, Results and Discussion

Measurements were made using the standard three-electrode configuration with working electrode, platinum counter electrode, and saturated calomel reference electrode. Photovoltage, capacity, and electroreflection measurements were made using lock-in techniques. Monochromatic light was provided by a halogen lamp (100 W) and a double-prism monochromator.

Quantum efficiency:

Fig. 4 shows the quantum efficiency for CdSiAs₂ and ZnSnP₂ in 1M H₂SO₄ uncorrected for reflection and electrolyte absorption losses. CdSiAs₂ has an efficiency between 50 and 60% over a broad spectral range for the polarization direction $\vec{E} \parallel \vec{c}$ where \vec{c} is the tetragonal axis. In the case of ZnSnP₂ the efficiency for non-polarized light is in the same order but with a slower increase for energies above the energy gap.

Energy gap:

The energy gap can be measured e.g. optically by an absorption measurement or by electrolyte electroreflectance (EER). In the latter the reflection is measured under the influence of the modulated electrical field in the space charge region. In

practice this is accomplished by modulating the electrode potential. The easiest way to apply this technique is based on the validity of the low-field approximation^[8].

In the low-field limit the electroreflectance signal can be described by the formula

$$\Delta R/R \approx (2 \cdot e \cdot N_A \cdot V_{SC}/\epsilon) \cdot L(h\nu) \quad (1)$$

where

$$L(h\nu) \approx \text{Re}(C \cdot e^{i\theta} \cdot (h\nu - E_g + i\Gamma)^{-n}) \quad (2)$$

V_{SC} is the fundamental harmonic component measured by phase-sensitive detection of the time-dependent potential $V(t)$. $L(h\nu)$ is a line-shape function describing the spectral dependence of the signal. As it can be seen in Equation (2) the electroreflectance signal depends among other things on the gap energy E_g . Aspnes has introduced a simple 3-point graphical technique for the determination of E_g from the EER spectrum^[8]. Applying this method for CdSiAs₂ a gap energy of 1.55 eV was found, while $E_g = 1.68$ eV in the case of ZnSnP₂. Both values are in good accordance with the literature where $E_g(\text{CdSiAs}_2) = 1.55$ eV and $E_g(\text{ZnSnP}_2) = 1.66$ eV^[7]. Fig. 5 shows an EER-spec-

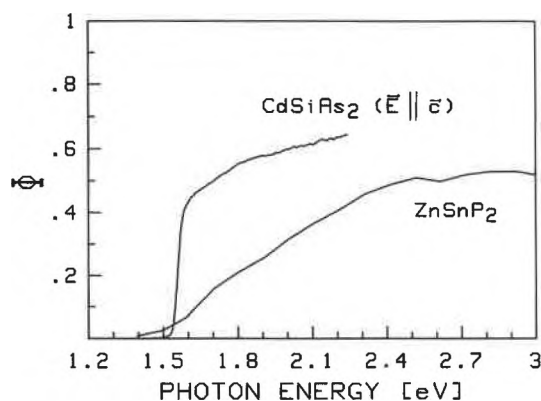


Fig. 4. Quantum yield spectra of CdSiAs₂ and ZnSnP₂ in 1M H₂SO₄. The CdSiAs₂ spectrum was measured with polarized light and $\vec{E} \parallel \vec{c}$, where \vec{c} is the tetragonal axis.

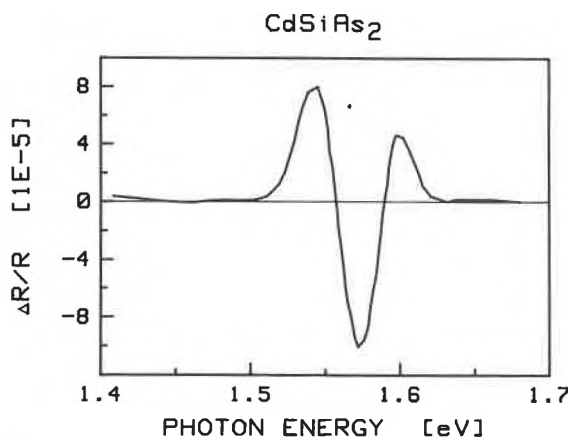


Fig. 5. Electrolyte-electroreflectance spectrum of CdSiAs₂ in 1M H₂SO₄ for $\vec{E} \parallel \vec{c}$. Modulation: 100 mVpp and 115 Hz. Electrode potential: $-0.2 V_{SCE}$.

trum of CdSiAs₂ in 1M H₂SO₄. The periodic change of the electric field was achieved by modulating the electrode potential with 100 mVpp around the bias of -0.2 V_{SCE}. The modulation frequency was 115 Hz.

Flatband potential:

The flatband can be measured by different methods like impedance measurement or EER measurement. The capacity of the space charge layer follows from complex impedance measurements after the analysis with a more or less simple equivalent circuit. The intersection of the 1/C² vs. potential plot with the potential axis leads to V_{fb} according to the Mott-Schottky theory^[9]:

$$1/C^2 = 2/(q \cdot N_{sc} \cdot \epsilon \cdot \epsilon_0 \cdot A^2) \cdot (V - V_{fb} - kT/q)$$

Fig. 6 shows Mott-Schottky plots for a CdSiAs₂ and a ZnSnP₂ electrode in 1M H₂SO₄ and a modulation frequency of 50 kHz. The modulation amplitude was 20 mVpp. For freshly etched CdSiAs₂ a flatband value of +0.22 V_{SCE} was found by extrapolation of the curves. A fast cathodic shift for the flatband to -0.2 V_{SCE} could be observed after the etching. Perfectly linear Mott-Schottky plots were obtained for frequencies from 700 Hz up to

70 kHz. Though the plots do show some frequency dependence which is mainly visible in the variation of the slopes, at steady state conditions the deduced flatband value remains nearly constant tending towards -0.2 V_{SCE} for frequencies higher than 5 kHz. The measurement for ZnSnP₂ over the same frequency range shows again a slight variation in the slopes but also no dependence in the evaluated «flatbands» which lie at +0.72 V_{SCE}.

Due to the obvious shortcomings of this technique an additional method for the determination of the flatband is preferable. This technique is again based on the EER measurement. Since the EER signal detected by the lock-in technique changes phase by 180 degrees compared with the modulation reference at the moment of flatband transition, a change of sign occurs^[10]. In the point-by-point method EER flatband determination was performed by measuring the EER spectra at different electrode potentials. The value of the highest peak in each spectrum was plotted as a function of the potential. In the other method, E_{phot} was set to the highest peak in the spectra and then the potential was swept slowly towards the flatband. Since the flatband condition could not be reached due to excessive anodic current, the resulting curve

did not exhibit a sign change. Approximate values for the flatband potential were found in both methods by extrapolating the decreasing part in the plots giving V_{fb} ≈ +0.3 V_{SCE} for CdSiAs₂ (Fig. 7). First measurements for ZnSnP₂ with the second method resulted in an approximate value of V_{fb} ≈ +0.7 V_{SCE} which corroborates again the value determined from the impedance measurements.

5. Conclusions and Outlook

In conclusion we can state that both materials CdSiAs₂ and ZnSnP₂ are attractive for further investigation for their suitability for photovoltaic devices. The direct bandgaps lie near the value for optimal conversion efficiency. The quantum efficiency exceeds 50% but with a slow increasing at the band edge in the case of ZnSnP₂. Flatband shift after etching the surface specially seen by CdSiAs₂ has to be inhibited perhaps by specific adsorption of positive ions. Due to this and the size of the gap which lies very near the optimum CdSiAs₂ is better suited for dry applications. The larger gap and the relatively high flatband potential make ZnSnP₂ to a promising candidate for photoelectrochemical energy conversion. It could be used, e.g. as a photocathode in a two-electrode photoelectrolysis cell (with an additional photoanode) or as a single photocathode with an additional external bias in photoassisted electrolysis.

The question whether photoelectrolysis will ever cover a significant part of the world energy needs still hinges upon the crucial problem to find efficient and stable electrode materials which can be manufactured at sufficiently low costs.

We would like to thank Dr. O. E. Hüßler for many valuable discussions and Mr. H. Gübeli for the technical assistance. Financial support of the Federal Office for Education and Science is gratefully acknowledged.

Received: January 19, 1988 [TR 26]

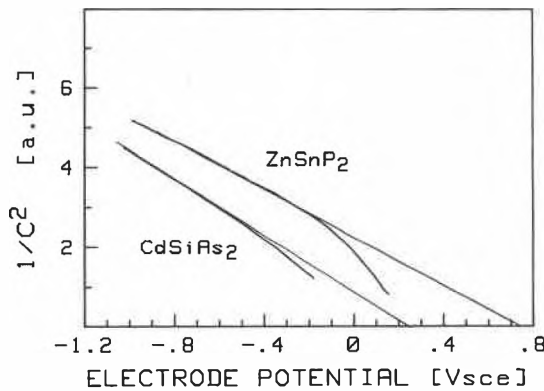


Fig. 6. Mott-Schottky plots in 1M H₂SO₄ for a ZnSnP₂ and a freshly etched CdSiAs₂ electrode. Modulation frequency was 50 kHz and the modulation amplitude 20 mVpp.

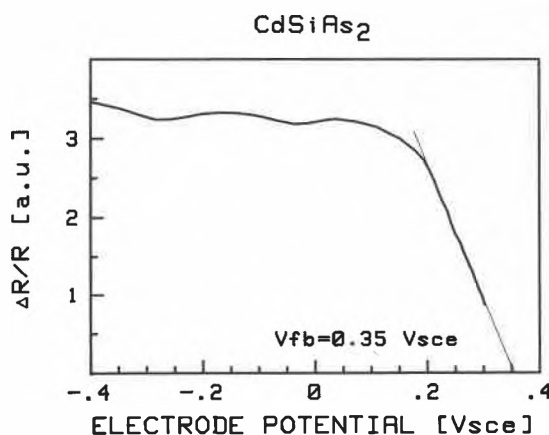


Fig. 7. Electrolyte-electroreflectance flatband plot in 1M H₂SO₄ for CdSiAs₂ at E_{phot} = 1.575 eV for E_{vec} || c̄. Modulation: 50 mVpp and 110 Hz.

[1] S. Stucki, *Chimia* 42 (1988) 94.
 [2] P. Suter, *Chimia* 42 (1988) 85.
 [3] J. J. Loferski, *J. Appl. Phys.* 27 (1956) 777.
 [4] R. Minder, M. Wolf, J.-R. Leidner, *Chimia* 42 (1988) 124.
 [5] M. F. Weber, M. J. Dignam, *Proc. 5th World Hydrogen Energy Conf. (Toronto)* 3 (1984) 657.
 [6] T. Cotting, H. von Känel, G. Leicht, H. Lévy, «Photoelectrochemical investigations of CdSiAs₂», *J. Electrochem. Soc.*, in press.
 [7] J. L. Shay, J. H. Wernick: *Ternary Chalcopyrite Semiconductors*, Pergamon Press, Oxford (1975).
 [8] D. E. Aspnes, in M. Balkanski (Ed.): *Handbook on Semiconductors*, North-Holland, Amsterdam (1980).
 [9] S. R. Morrison: *Electrochemistry at Semiconductor and Oxidized Metal Electrodes*, Plenum, New York (1980).
 [10] T. Cotting, H. von Känel, *Surf. Sci.* 162 (1985) 796.